

Thermoelasticity of damaged elastomers - symmetry issues

To cite this article: M V Micunovic *et al* 2007 *J. Phys.: Conf. Ser.* **62** 88

View the [article online](#) for updates and enhancements.

Related content

- [Composite Materials: Computing exact relations and links †](#)
Y Grabovsky
- [Closed solutions for model problems in generalized thermoelasticity](#)
S. A. Lychev and V.V. Klindukhov
- [Electromechanical response of silicone dielectric elastomers](#)
V Cârlescu, G Priscaru and D Olaru

Recent citations

- [On inelasticity of damaged quasi rate independent anisotropic materials](#)
Milan Miunović and and Ljudmila Kudrjavceva
- [Thermoelasticity of Damaged Elastomers by Self-consistent Method](#)
M. Miunovi *et al*



IOP | ebooks™

Bringing you innovative digital publishing with leading voices to create your essential collection of books in STEM research.

Start exploring the collection - download the first chapter of every title for free.

Thermoelasticity of damaged elastomers - symmetry issues

M V Micunovic¹, L T Kudrjavceva² and D Sumarac³

^{1,2} Faculty of Mechanical Engineering, University of Kragujevac, Sestre Janjica 6, 34000 Kragujevac, Serbia

³ Faculty of Civil Engineering, University of Belgrade, Kralja Aleksandra 70, Serbia

E-mail: mmicun@kg.ac.yu

Abstract. The paper deals with an elastomer body having a random 3D-distribution of two phase inclusions: spheroidal mutually parallel voids as well differently oriented reinforcing parallel elastomeric stiff spheroidal short fibers. By the effective field approach the effective stiffness 4-tensor as well as the effective thermal expansion 2-tensor are formulated and found numerically. Simultaneous and sequential embeddings of inclusions are compared. Special attention is paid to the problem of effective elastic and thermal symmetry. The results of the theory are applied to two families of inclusions (having either prolate fibres or oblate voids).

Keywords: Elastic and thermal effective anisotropy, self consistent effective field method, Eshelbian implants.

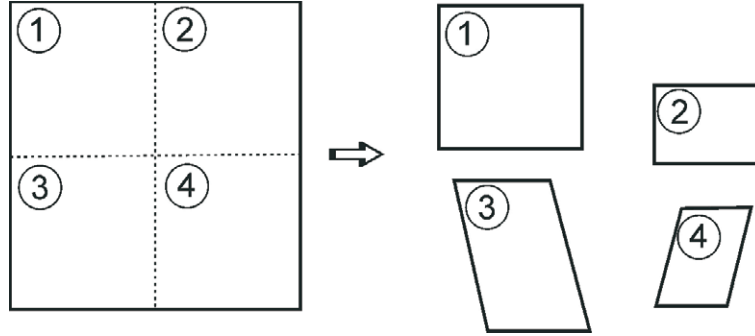
1. Introduction

Classical texts devoted to the continuum theory of dislocations as the principal source of residual stresses consider incompatibility of either plastic strains or quasi-plastic strains (thermal and some others). An elementary visualization of eigenstrains caused by such an incompatibility is given in figure 1(a). The key point is that if volume elements in the natural state space (of Kondo [13]) deform freely then they cannot be connected without residual stresses. While such an approach (promoted originally by Kröner [15]) looked very promising in plasticity based on continuum dislocations, recent papers mainly use implantations as proposed by Eshelby [6]. A simplified picture of such an approach is depicted in figure 1(b). The Eshelbian approach is especially suitable for description of composites with particulate phases such as either stiff or soft inclusions.

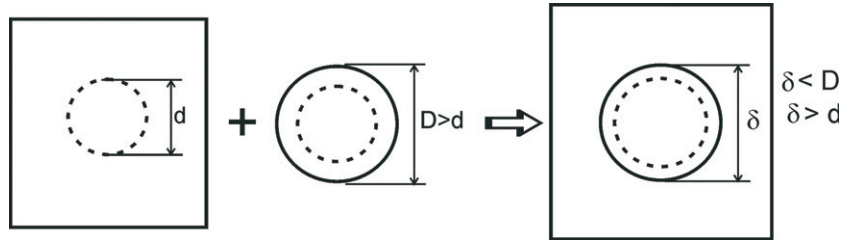
It should be noted that in papers dealing with particulate composites using the Eshelbian self consistent approach one of the following intrinsic geometries is commonly accepted:

- inclusions are spherical;
- inclusions are ellipsoidal with random orientations leading to isotropy and
- inclusions are ellipsoidal with parallel semi-axes.

All these topologies are artificial and not realistic. Their advantage is that they allow for easy and explicit account of simple material symmetry. In fact under multiaxial and, often, nonproportional stress states voids either open or close and inclusions rotate. Such intrinsic reorganizations cause complicated dynamical material symmetries.



(a) Incompatibility of strains in natural state space of Kondo.



(b) Eshelby's implanting eigenstrain by the same material of inclusion and matrix.

Figure 1. Two types of imperfections causing residual stresses.

Our aim in this paper is to analyze elastomeric composites possessing voids and reinforced by short cylindrical fibres. Such materials have become indispensable as vibration absorbing supports of railway tracks. They will be modeled here by many groups of ellipsoidal inclusions. In each group all the inclusions are presumably identical - made of the same material with parallel semi-axes.

To realize this aim we first briefly review some existing self-consistent theories of elastic composites with multiphase structure ([9, 10, 12, 11, 22, 31]). Then effective thermal expansion tensor for three phase composites is derived based on papers [19, 20] and the monograph [11] where two phase composites were considered. In the last section we determine numerically effective elastic stiffness as well as effective thermal expansion for some composites with specially disoriented inclusions.

In this paper, like in [12], we assume that the considered composite is composed of three isotropic phases: elastomeric matrix, spheroidal voids and spheroidal stiff polymer inclusions. Each class of inclusions contains parallel but randomly distributed spheroids.

Before addressing the issues listed above we recall briefly how Eshelby defined his tensor in the case of isotropic materials.

1.1. Eshelbian approach to eigenstrains

According to Mura [30] constrained implanting strains induced by free strains are termed as "eigen-strains". Constrained and free strains are connected by the known Eshelby formula [6]:

$$\boldsymbol{\epsilon}^{constr} = \mathcal{S}\boldsymbol{\epsilon}^{free}. \quad (1)$$

In the above formula the unconstrained strain $\boldsymbol{\epsilon}^{free}$ (strain in the middle of figure 1(b)) is related to implanting "eigen-strain" (strain on RHS of figure 1(b)) by the fourth rank tensor \mathcal{S} . In the special case of the same isotropic materials of matrix and inclusion Eshelby's 4-tensor reads

(capital and small indices take the same values but there is no summation over repeated capital and small indices):

$$\begin{aligned} \frac{8\pi(1-\nu)}{3} S_{mnkl} &= \left(I_{MK} a_K^2 - I_M \varsigma \right) \delta_{mn} \delta_{kl} + \\ &\quad \left(\frac{a_M^2 + a_N^2}{2} I_{MN} + \frac{I_M + I_N}{2} \varsigma \right) (\delta_{mk} \delta_{nl} + \delta_{nk} \delta_{ml}), \end{aligned}$$

with notations $\varsigma \equiv (1 - 2\nu)/3$,

$$I_M = \lim_{\xi \rightarrow 0} \int_{\xi}^{\infty} \frac{d\xi}{(a_M^2 + \xi)\Delta}, \quad I_{MN} = \lim_{\xi \rightarrow 0} \int_{\xi}^{\infty} \frac{d\xi}{3(a_M^2 + \xi)(a_N^2 + \xi)\Delta}$$

and $\Delta^2 \equiv (a_1^2 + \xi)(a_2^2 + \xi)(a_3^2 + \xi)(2\pi a_1 a_2 a_3)^{-2}$. The components of \mathcal{S} are presented in Figs. 2(a) and 2(b) for an isotropic material. On the other hand, in the case of a general anisotropic material a numerical estimation is the only way to calculate \mathcal{S} . Whenever the considered matrix is anisotropic the formula of Kunin & Sosnina [18] must be applied in the way explained by Yaguchi & Busso [35]. For some anisotropic materials these figures have a form depending on the stiffness tensor and orientation of the considered ellipsoidal inclusion (according to equation (6) given below).

2. Effective properties tensors

Let stiffness and its inverse be denoted by \mathcal{D}_{Λ} , $\mathcal{M}_{\Lambda} \equiv \mathcal{D}_{\Lambda}^{-1}$, ($\Lambda \in \{0, c, f\}$) for matrix, voids and fibers respectively. Then by means of the notation $\delta\mathcal{D}(x) \equiv \mathcal{D}(x) - \mathcal{D}_0$, $\delta\mathcal{M}(x) \equiv \mathcal{M}(x) - \mathcal{M}_0$, and by the characteristic function

$$V(x) = \sum_{k=1}^N V_k(x) = \begin{cases} 1, & x \in V, \\ 0, & x \notin V, \end{cases}$$

for N inclusions we have

$$\boldsymbol{\varepsilon}(x) = \boldsymbol{\varepsilon}_0 - \mathcal{K}_0^{\varepsilon} * (\delta\mathcal{D} \boldsymbol{\varepsilon} V), \quad (2)$$

$$\boldsymbol{\sigma}(x) = \boldsymbol{\sigma}_0 + \mathcal{K}_0^{\sigma} * (\delta\mathcal{M} \boldsymbol{\sigma} V) \quad (3)$$

where $(\mathcal{K} * \mathcal{A})(x) \equiv \int \mathcal{K}(x-y) \mathcal{A}(y) dy$.

The above two kernels are introduced by means of a Green's function of the matrix \mathbf{G}_0 using Kunin's notation [17] $\mathcal{K}_0^{\varepsilon} \equiv -def \mathbf{G}_0 def$ and $\mathcal{K}_0^{\sigma} = \mathcal{D}_0 \mathcal{K}_0^{\varepsilon} \mathcal{D}_0 - \mathcal{D}_0 \delta(x)$ where the total (linear) strain expressed by the displacement reads $\boldsymbol{\varepsilon} = def \mathbf{u}$ and $\delta(x)$ is the Dirac delta function.

2.1. Effective stiffness

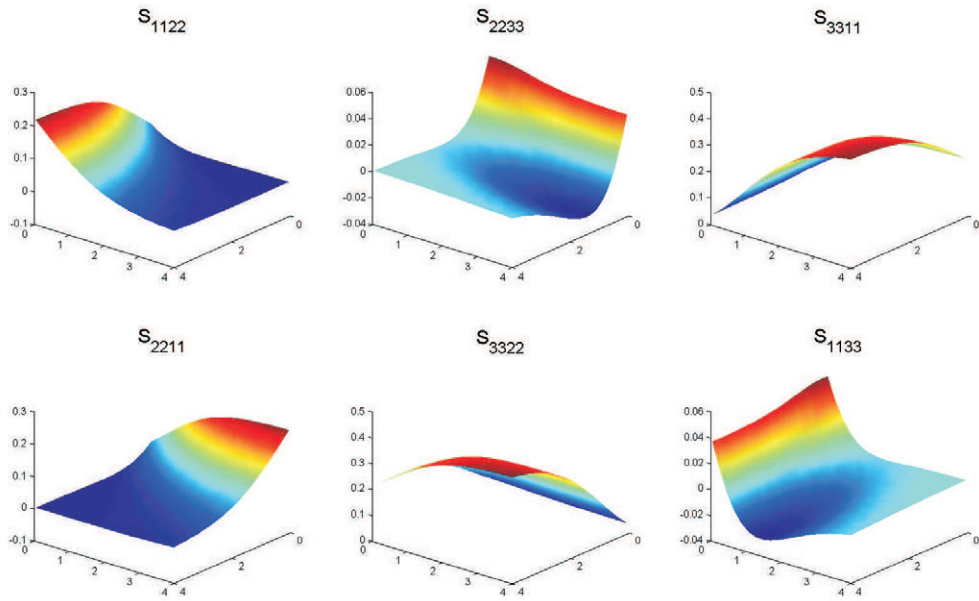
An effective stiffness tensor is defined by spatial averaging as follows. The micro formulation of Hooke's law in the case of a thermoelastic deformation leads to the definition of the effective stiffness:

$$\langle \boldsymbol{\sigma} \rangle = \mathcal{D}^{eff} \langle \boldsymbol{\varepsilon}_e \rangle$$

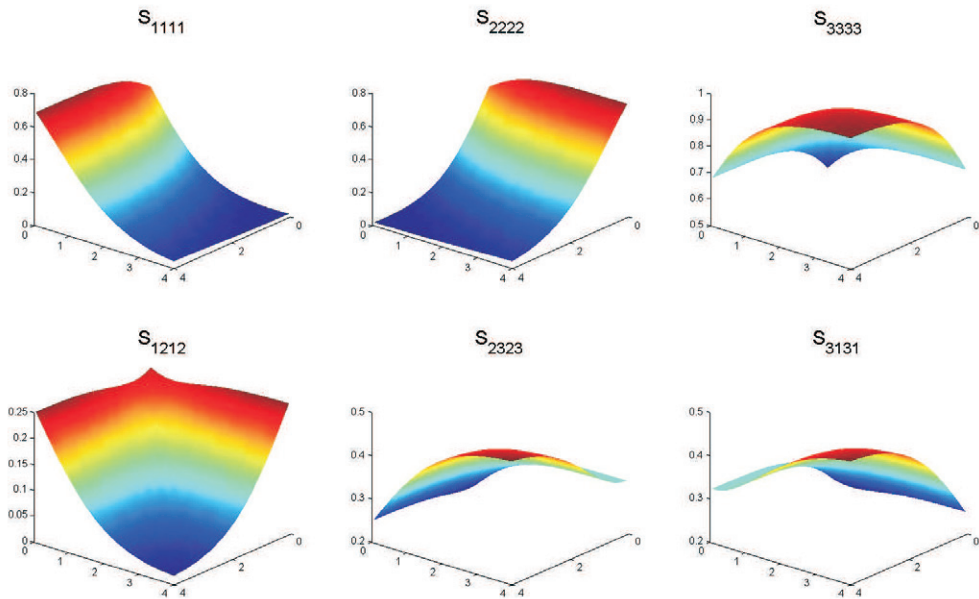
where $\boldsymbol{\varepsilon}_{ke} = \boldsymbol{\varepsilon}_k - \boldsymbol{\alpha}_k \theta$ for a point $x \in V_k$ and $\langle \mathcal{F} \rangle := 1/V \int_V \mathcal{F}(x) dx$ due to the ergodic hypothesis.

Introducing the notation

$$\boldsymbol{\varepsilon}_*(x_k) := \boldsymbol{\varepsilon}_0 - \sum_{m \neq k} \mathcal{K}_0^{\varepsilon} * (\delta\mathcal{D} \boldsymbol{\varepsilon} V_m) \quad (4)$$



(a) Pair off-diagonal components



(b) Diagonal and pair-screw components.

Figure 2. Components of the Eshelby tensor for logarithms of diverse principal axes ratios for isotropic materials.

we may write for a k -th inclusion a nonlocal formula which has the same form as the

corresponding formula for a continuum with a single inclusion i.e.:

$$\boldsymbol{\varepsilon}(x_k) + \int_{V_k} \mathcal{K}_0^\varepsilon(x - x') \delta \mathcal{D}(x') \boldsymbol{\varepsilon}(x') dx' = \boldsymbol{\varepsilon}_*(x_k). \quad (5)$$

The two principal hypotheses of the *effective field method* are [11, 22]:

HYPOTHESIS 1 $\boldsymbol{\varepsilon}_*(x) = \text{const}$ for small $|x - x_k|$ and

HYPOTHESIS 2 $\boldsymbol{\varepsilon}_*(x_k)$ is statistically independent of the elastic properties of the medium and shape of the inclusion V_k .

Moreover, the quasi-crystallinity assumption of Lax [22] states that $\boldsymbol{\varepsilon}_*(x) = \text{const}$ for all points inside the considered *representative volume element* (RVE)¹. Then, due to linearity of the governing equations it is possible to write:

$$\boldsymbol{\varepsilon}(x) = \mathcal{L}_k(x) \boldsymbol{\varepsilon}_*, \quad \text{for } x \in V_k,$$

where, for the k -th inclusion $\mathcal{L}_k = (\mathcal{I} + \mathcal{A}_k \delta \mathcal{D}_k)^{-1}$ with

$$\mathcal{A}_k = \int_{V_k} \mathcal{K}_0^\varepsilon(x) dx \equiv \mathcal{S}(a_k) \mathcal{D}_0^{-1} \quad (6)$$

where $\mathcal{S}(a_k)$ is the Eshelby 4-tensor for the considered inclusion. Introduce a *correlation function* by means of [11]

$$\mathcal{A}^\Phi = \int \mathcal{K}_0^\varepsilon(x) \Phi(x) dx, \quad (7)$$

where c is concentration of inclusions and the scalar function

$$\Phi(x - x') := 1 - \frac{1}{c} \left\langle \sum_{m \neq k} V_m(x') |x \right\rangle, \quad x \in V_k$$

obtained by averaging is defined by the shape of the correlation hole. This leads to the effective stiffness for a single family of inclusions (built by the same material):

$$\mathcal{D}^{eff} = \mathcal{D}_0 + c(\langle \delta \mathcal{D} \mathcal{L} \rangle^{-1} - c \mathcal{A}^\Phi)^{-1}. \quad (8)$$

If all the inclusions are the same (shape, orientation and elastic properties) with $\mathcal{A}_k \equiv \mathcal{A}(a)$ then (8) simplifies into:

$$\mathcal{D}^{eff} = \mathcal{D}_0 + c(\delta \mathcal{D}^{-1} + \mathcal{A}(a) - c \mathcal{A}^\Phi)^{-1}, \quad (9)$$

which in the most special case when $\mathcal{A}(a) = \mathcal{A}^\Phi$ (correlation gap and the inclusion have same aspect ratios) leads to the Mori-Tanaka formula [12].

In an extension of results of Kanaun and Levin, [11], to the case of finite number N of ellipsoidal inclusions Markov [22] has derived the following set of formulae

$$(\mathcal{I} + \mathcal{A}_k \delta \mathcal{D}_k) \boldsymbol{\varepsilon}_{(k)} - \sum_{s=1}^N c_{(s)} \mathcal{A}_{ks} \delta \mathcal{D}_s \boldsymbol{\varepsilon}_{(s)} = \boldsymbol{\varepsilon}_0, \quad k \in \{1, \dots, N\} \quad (10)$$

$$\langle \boldsymbol{\varepsilon} \rangle = (1 - \sum_{s=1}^N c_{(s)}) \boldsymbol{\varepsilon}_0 + \sum_{s=1}^N c_{(s)} \boldsymbol{\varepsilon}_{(s)}, \quad (11)$$

¹ Size of RVE is discussed in [27].

$$\langle \boldsymbol{\sigma} \rangle = \mathcal{D}^{eff} \langle \boldsymbol{\varepsilon} \rangle = \mathcal{D}_0 \langle \boldsymbol{\varepsilon} \rangle + \sum_{s=1}^N c_{(s)} \delta \mathcal{D}_s \boldsymbol{\varepsilon}_{(s)}. \quad (12)$$

The linearity of (10) leads to the solution $\boldsymbol{\varepsilon}_{(k)} = \mathcal{F}_k \boldsymbol{\varepsilon}_0$, $k \in \{1, \dots, N\}$ which inserted into (12) leads to the effective stiffness tensor \mathcal{D}^{eff} . The principal problem, however, is to determine mutual (pair) correlation tensors \mathcal{A}_{ks} . Such tensors were calculated in [31] under the hypothesis of ellipsoidal symmetry for the distribution of the inclusions and the integration ellipsoids exclude overlapping of ellipsoidal inclusions. Explicit results were given for spheroidal inclusions immersed into an isotropic matrix.

In a recent paper Kanaun and Jeulin [12] considered pure elasticity of a composite with an isotropic matrix possessing two families of mutually parallel inclusions (spheroids and cylinders). We will adapt their results to our subject of interest: prolate spheroidal voids and oblate spheroidal fibres (denoted by indices c and f respectively). Their analysis prefers a Boolean distribution of inclusions and they considered two typical cases of generation priority:

- Simultaneous generation of both families when one family has priority. In our case it is logical for the fibres to have priority since voids could not introduce restriction on fibre appearance. Their stiffness tensor reads:

$$\mathcal{D}^{eff} = \mathcal{D}_0 + c_{*c} \mathcal{T}_c \mathfrak{T}_c + c_{*f} \mathcal{T}_f \mathfrak{T}_f, \quad (13)$$

with concentrations $c_{*c} = c_c(1 - c_f)$, $c_{*f} = c_f$, $q = 1 - c_c/(1 - c_f)$ and

$$\left. \begin{aligned} \mathcal{T}_\Lambda^{-1} &= \delta \mathcal{D}_\Lambda^{-1} + \mathcal{A}_\Lambda, \\ \mathcal{L}_\Lambda &= \mathcal{I} + c_{*\Lambda} (\mathcal{A}_{\Lambda\Lambda}^\Phi - \mathcal{A}_{c_f}^\Phi) \mathcal{T}_\Lambda, \end{aligned} \right\} \Lambda \in \{c, f\},$$

$$\mathfrak{T}_\Lambda = (\mathcal{I} - c_{*\Lambda} \mathcal{A}_{\Lambda\Lambda}^\Phi \mathcal{T}_\Lambda - c_{*\Pi} \mathcal{A}_{c_f}^\Phi \mathcal{T}_\Pi \mathcal{L}_\Pi^{-1} \mathcal{L}_\Lambda)^{-1}, \quad (\Lambda, \Pi) \in \{(c, f), (f, c)\}.$$

Here in the correlation 4-tensors

$$\mathcal{A}_{\Lambda\Pi}^\Phi = \int \mathcal{K}_0^\varepsilon(x) \Phi_{\Lambda\Pi}(x) dx, \quad (\Lambda, \Pi) \in \{(c, c), (f, f), (c, f)\}, \quad (14)$$

$$\Phi_{km}(x - x') := 1 - \frac{1}{c_k} \langle \sum_{m \neq k} V_m(x') | x \in V_k \rangle, \quad V_k \in V_\Lambda, V_m \in V_\Pi,$$

for spheroidal shapes of both types of inclusions, the Boolean scalar functions are:

$$\Phi_{ff}(r) = 1 - \frac{1}{c_f^2} [1 - (1 - c_f)^{1-H_f(r)}]^2 (1 - c_f)^{H_f(r)}, \quad (15)$$

$$\Phi_{cc}(r) = 1 - \frac{1}{c_c^2} [1 - q^{1-H_c(r)}]^2 q^{H_f(r)} (1 - c_f)^{2-H_f(r)}, \quad (16)$$

$$\Phi_{cf}(r) = \Phi_{fc}(r) = 1 - \frac{1}{c_f} [1 - (1 - c_f)^{1-H_f(r)}], \quad (17)$$

with $H_\Lambda = 1 - N/(N-1)r/2 + 1/(N-1)(r/2)^N$, $r < 2$, ($N = 3$). For some values (say $c_f = 0.4$, $c_c = 0.2$) these functions are shown on the next figure Their meaning is very close to the correlation functions used in [31].

- Sequential generation when the second family of voids is delayed after the Boolean generation of fibres. As the authors in [12] pointed out, such an order is recommended when fibre concentration c_f is considerably larger than void concentration c_c . In this case the determination of effective stiffness is given by a two-step procedure:

$$\mathcal{D}_c^{eff} \equiv \mathcal{D}_0 + c_{*c} (\mathcal{D}_c^{-1} - \mathcal{D}_0^{-1} + \mathcal{A}(a_c) - c_{*c} \mathcal{A}_{cc}^\Phi)^{-1}, \quad (18)$$

$$\mathcal{D}^{eff} = \mathcal{D}_c^{eff} + c_{*f} (\mathcal{D}_f^{-1} - (\mathcal{D}_c^{eff})^{-1} + \mathcal{A}(a_f) - c_{*f} \mathcal{A}_{ff}^\Phi)^{-1}. \quad (19)$$

Some applications of both approaches to a composite with short fibres and voids will be given in the last section of this paper.

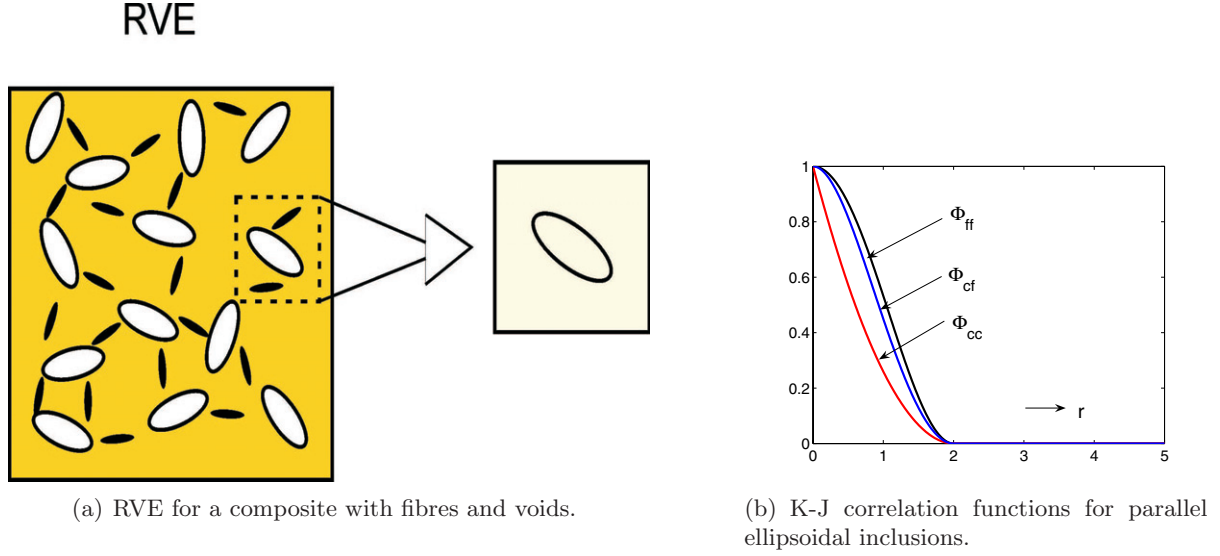


Figure 3. Notion of the representative volume element and Kanaun-Jeulin interactions.

2.2. Tensor of effective thermal expansion coefficients

While in the previous subsection elasticity without thermal effects is analyzed, the subject of this subsection is the thermoelasticity of composites with two families of ellipsoidal inclusions. The procedure mainly follows [11] and [10] where spherical inclusions are treated. First, let us introduce the notion of stress on an inclusion exerted by all the others:

$$\sigma_*(x_k) := \sigma_0 - \sum_{m \neq k} \mathcal{K}_0^\sigma * (\delta \mathcal{M} \sigma V_m + \delta \alpha \theta V_m) \quad (20)$$

Then stress in a k -th inclusion has the same form as the corresponding formula for a continuum with a single inclusion ($x \in V_k$) i.e.:

$$\sigma(x) + \int_{V_k} \mathcal{K}_0^\sigma(x-x') (\delta \mathcal{M}(x') \sigma(x') + \delta \alpha(x') \theta(x')) dx' = \sigma_*. \quad (21)$$

If we look at a composite with a single inclusion, then the following tensors are important:

$$\begin{aligned} \mathcal{Q}_k &\equiv \mathcal{D}_0 - \mathcal{D}_0 \mathcal{A}_k \mathcal{D}_0, \\ \mathcal{L}_\Lambda^\sigma &= (\delta \mathcal{M}_\Lambda^{-1} + \mathcal{Q}_\Lambda)^{-1}, \quad \text{with} \quad \overline{\mathcal{L}}_\Lambda^\sigma \equiv \langle \mathcal{L}_\Lambda^\sigma \rangle |_\Lambda, \\ \mathbf{I}_\Lambda^\theta &= (\mathcal{I} - \mathcal{L}_\Lambda^\sigma \mathcal{Q}_\Lambda) \delta \alpha_\Lambda, \quad \text{with} \quad \overline{\mathbf{I}}_\Lambda^\theta \equiv \langle \mathbf{I}_\Lambda^\theta \rangle |_\Lambda, \end{aligned} \quad (22)$$

where $\langle \bullet \rangle |_\Lambda := 1/V_\Lambda \int_{V_\Lambda} \bullet(x) dx$ and $\mathcal{A}_k = \mathcal{S}(a_k) \mathcal{D}_0^{-1}$ as in (6).

Let us turn now our attention to the case of a composite with fibres and voids. In the sequel we follow exactly the procedure explained in [11] extending their analysis to the case of two classes of inclusions. First, instead of (20) we calculate stresses at a point ($x \in V_k$) exerted by only one class of inclusions i.e.:

$$\begin{aligned} \sigma_{*f} &= (\mathfrak{B}_{fc}^{-1} \mathfrak{B}_{ff} - \mathfrak{B}_{cc}^{-1} \mathfrak{B}_{cf})^{-1} (\mathfrak{B}_{cc}^{-1} \beta_c - \mathfrak{B}_{fc}^{-1} \beta_f) \theta \equiv \mathbf{L}_f^\theta \theta, \\ \sigma_{*c} &= (\mathfrak{B}_{cf}^{-1} \mathfrak{B}_{cc} - \mathfrak{B}_{ff}^{-1} \mathfrak{B}_{fc})^{-1} (\mathfrak{B}_{ff}^{-1} \beta_f - \mathfrak{B}_{cf}^{-1} \beta_c) \theta \equiv \mathbf{L}_c^\theta \theta, \end{aligned} \quad (23)$$

where:

$$\begin{aligned}\beta_{*f} &= c_f \overline{\mathbf{1}}_f^\theta \mathcal{B}_{ff}^\Phi + c_c \overline{\mathbf{1}}_c^\theta \mathcal{B}_{fc}^\Phi, \\ \beta_{*c} &= c_f \overline{\mathbf{1}}_f^\theta \mathcal{B}_{cf}^\Phi + c_c \overline{\mathbf{1}}_c^\theta \mathcal{B}_{cc}^\Phi\end{aligned}\quad (24)$$

and

$$\begin{aligned}\mathfrak{B}_{ff} &= \mathcal{I} + c_f \mathcal{B}_{ff}^\Phi \mathcal{L}_f^\sigma, & \mathfrak{B}_{fc} &= c_c \mathcal{B}_{fc}^\Phi \mathcal{L}_c^\sigma, \\ \mathfrak{B}_{cf} &= c_c \mathcal{B}_{cf}^\Phi \mathcal{L}_f^\sigma, & \mathfrak{B}_{cc} &= \mathcal{I} + c_c \mathcal{B}_{cc}^\Phi \mathcal{L}_c^\sigma,\end{aligned}\quad (25)$$

Herein instead of (14) we use the stress correlation functions :

$$\mathcal{B}_{\Lambda\Pi}^\Phi = \int \mathcal{K}_0^\sigma(x) \Phi_{\Lambda\Pi}(x) dx, \quad (\Lambda, \Pi) \in \{(c, c), (f, f), (c, f)\}.\quad (26)$$

based on the stress kernel \mathcal{K}_0^σ . Now, inserting both stresses σ_{*f} and σ_{*c} into (21) and performing corresponding integrations we arrive at:

$$\alpha^{eff} = \alpha_0 + \overline{\mathbf{1}}_f^\theta + \overline{\mathbf{1}}_c^\theta + \overline{\mathcal{L}}_f^\sigma \mathbf{L}_f^\theta + \overline{\mathcal{L}}_c^\sigma \mathbf{L}_c^\theta.\quad (27)$$

For the undamaged composite without voids inserting $c_c = 0$, $\delta\mathcal{M}_c = 0$ and $\delta\alpha_c = 0$ the above formula simplifies into the form

$$\alpha^{eff} = \alpha_0 + \overline{\mathbf{1}}_f^\theta + \overline{\mathcal{L}}_f^\sigma \mathbf{L}_f^\theta\quad (28)$$

derived in the book [11].

3. Anisotropy caused by presence of ellipsoidal inclusions

Material symmetry group \aleph of an elastic anisotropic material with Hooke's tensor \mathcal{D} is defined by all orthogonal 2-tensors satisfying the relationship: $\mathcal{D} = \mathbf{H} \diamond \mathcal{D}$, ($\mathbf{H} \in \aleph$), where the Rayleigh product explicitly reads: $(\mathbf{H} \diamond \mathcal{D})_{klmn} \equiv (\mathbf{H})_{ka}(\mathbf{H})_{lb}(\mathbf{H})_{mc}(\mathbf{H})_{nd}(\mathcal{D})_{abcd}$. A similar relationship holds true for the thermal expansion tensor. We state now the problem of overall symmetry for a representative volume element.

Overall symmetry definition

Given elastic and thermal symmetries of the matrix and N ellipsoidal inclusions (whose semiaxes are defined by the rotation tensors \mathbf{R}_Λ) as follows: $\mathcal{D}_\Lambda = \mathbf{H}_\Lambda^e \diamond \mathcal{D}_\Lambda$, $\mathbf{H}_\Lambda^e \in \aleph_\Lambda^e$, as well as $\alpha_\Lambda = \mathbf{H}_\Lambda^t \diamond \alpha_\Lambda$, $\mathbf{H}_\Lambda^t \in \aleph_\Lambda^t$, ($\Lambda \in \{0, 1, \dots, N\}$) find 2-tensors $\mathbf{H}_{eff}^e \in \aleph_{eff}^e$ and $\mathbf{H}_{eff}^t \in \aleph_{eff}^t$ such that

$$\mathcal{D}_{eff} = \mathbf{H}_{eff}^e \diamond \mathcal{D}_{eff}, \quad \mathbf{H}_{eff}^e \in \aleph_{eff}^e\quad (29)$$

as well as

$$\alpha_{eff} = \mathbf{H}_{eff}^t \diamond \alpha_{eff}, \quad \mathbf{H}_{eff}^t \in \aleph_{eff}^t\quad (30)$$

hold. Groups \aleph_{eff}^e and \aleph_{eff}^t are then called *effective elastic symmetry group* and *effective thermal symmetry group* respectively.

Obviously, the real task is to find \aleph_{eff}^e and \aleph_{eff}^t when \aleph_Λ^e and \aleph_Λ^t , ($\Lambda \in \{0, 1, \dots, N\}$), are given. To solve this problem, an appealing and simple approach would be to use the *orientation distribution function* ω (ODF) as follows (following [29]):

$$\langle F \rangle = \int_{SO(3)} F(\mathbf{R}) \omega(\mathbf{R}) d\aleph, \quad F \equiv \langle F \rangle + \delta F, \quad F \in \{\mathcal{D}, \sigma, \varepsilon\}.\quad (31)$$

Then using the definition of the effective stiffness tensor, the above decompositions to mean values and fluctuations lead to the expression for the effective stiffness:

$$\mathcal{D}^{eff} = \langle \mathcal{D} \rangle + \langle \delta \mathcal{D} \delta \varepsilon \rangle \langle \varepsilon \rangle^{-1}.\quad (32)$$

Explicit structure of (32) depends on topology and materials of matrix and inclusions. However, in all the cases (cf. (8, 13)) we have the dependence

$$\mathcal{D}^{eff}(\mathcal{D}_0, \omega(\mathbf{R}), a_1, \dots, a_N, \mathbf{R}_1, \dots, \mathbf{R}_N)$$

as it should be expected. For calculation of the above indicated mean values of strain and stiffness the usual procedure is to develop the ODF function into a series over generalized spherical functions as follows [32]:

$$\omega(\mathbf{R}) = \sum_{k=0}^{\infty} \sum_{m=-k}^{m=k} \sum_{n=-k}^{n=k} c_{kmn} P_{kmn}(\cos \theta) \exp(-im\varphi) \exp(-in\psi), \quad (33)$$

where P -functions are calculated by means of:

$$P_{kmn}(x) = \frac{(-1)^{k-m} i^{n-m}}{2^k (k-m)!} \sqrt{\frac{(k-m)!(k+n)!}{(k+m)!(k-n)!}} (1-x)^{-\frac{n-m}{2}} (1+x)^{-\frac{n+m}{2}} \times \frac{d^{k-n}}{dx^{k-n}} \left[(1-x)^{k-m} (1+x)^{k+m} \right]. \quad (34)$$

In the special case when ODF depends only on one angle, say θ , averaging over the other two Euler angles leads to the representation

$$\omega(\mathbf{R}) = \sum_{k=0}^{\infty} c_{2k} P_{2k}(\cos \theta), \quad (35)$$

where P_k , $k \in \{0, 2, 4, \dots\}$ with values $P_0(x) = 1$, $P_2(x) = (3x^2 - 1)/2$, $P_4(x) = (35x^4 - 30x^2 + 3)/8$, $P_6(x) = (231x^6 - 315x^4 + 105x^2 - 5)/16, \dots$ are Legendre functions of even order.

Before proceeding with general symmetry issues, let us consider now some characteristic distributions of inclusions immersed into a elastomer matrix. While orientations and shapes of inclusions of constituting diverse subgroups are fixed, their translational distributions inside each subgroup are random. Concerning orientations, figure 4(a) shows the first octant part of an ellipsoidal inclusion with semiaxis lengths a_1, a_2, a_3 . When all the inclusions are neither parallel nor fully random correlation 4-tensors (14) require specification of the corresponding functions (15-17). A simple approach to this problem is illustrated by figure 4(b) where one ellipsoidal inclusion is circumvented by non-overlapping inclusions of the other group. When range of interaction is generated by the form of the minimal non-overlapping central surface and the decrease of $\Phi_{\Lambda\Pi}$ inside the shadowed region is assumed to be linear we obtain the correlation tensors $\mathcal{A}_{\Lambda\Pi}$ by numerical integration.

For the sake of a simple estimation of anisotropy degree induced by inclusions let us introduce the *anisotropy factor* ζ defined by:

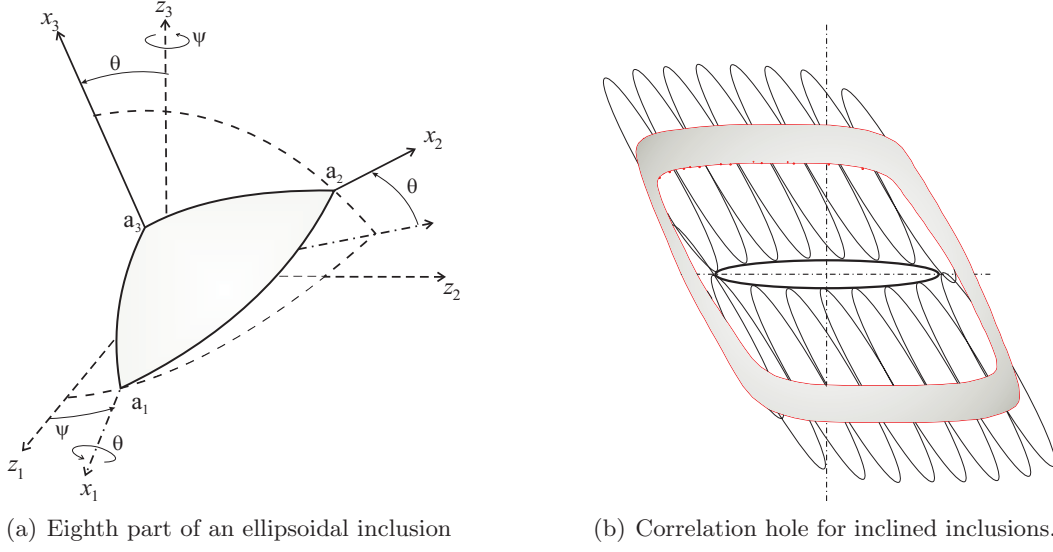
$$\zeta := \frac{\|\mathcal{D}_{an}^{eff}\|}{\|\mathcal{D}_{iso}^{eff}\|}, \quad (36)$$

where by means of the identity 2-tensor \mathbf{I} and 4-tensor \mathcal{I} (satisfying $\mathbf{I}\mathbf{A} = \mathbf{A}$ and $\mathcal{I}\mathcal{A} = \mathcal{A}$) we have the decomposition of the effective stiffness into its isotropic and anisotropic part (cf. [5]):

$$\mathcal{D}^{eff} = K^{eff} \mathbf{I} \otimes \mathbf{I} + 2\mu^{eff} \mathcal{I} + \mathcal{D}_{an}^{eff} \equiv \mathcal{D}_{iso}^{eff} + \mathcal{D}_{an}^{eff}. \quad (37)$$

Herein K^{eff} is the effective bulk modulus and μ^{eff} is the effective shear modulus.²

² A more detailed judgement of type of the anisotropy requires either Schouten's harmonic decomposition of the 4-tensor of effective stiffness or analysis of eigenvectors and eigenvalues of the corresponding 6×6 effective stiffness matrix.



(a) Eighth part of an ellipsoidal inclusion

(b) Correlation hole for inclined inclusions.

Figure 4. Correlation hole for inclined inclusions parallel inside each family.*Example 1.*

First, suppose that an elastomeric matrix is weakened by some identical parallel spheroidal voids with symmetry axis aligned with a Cartesian axis $z_3 = x_3$. Suppose now that two thirds of the voids are rotated by some angle θ_1 around axis z_1 whereas the remaining one third is rotated by $\theta_2 = -\theta_1 = \pi/6$ around the same axis. The angles $\psi_1 = \psi_2 = 0$ on the figure 4(a) and concentrations of voids $c_{c1} = 2c_{c2}$. The aspect ratios are the same: $\gamma_{c1} = \gamma_{c2} = a_1/a_3 = a_2/a_3$. In this way we obtain a composite with planar symmetry with mirror axis $x_1 = z_1$ and one family of voids with two subfamilies of parallel identical voids. Otherwise voids inside each subgroup are randomly distributed.

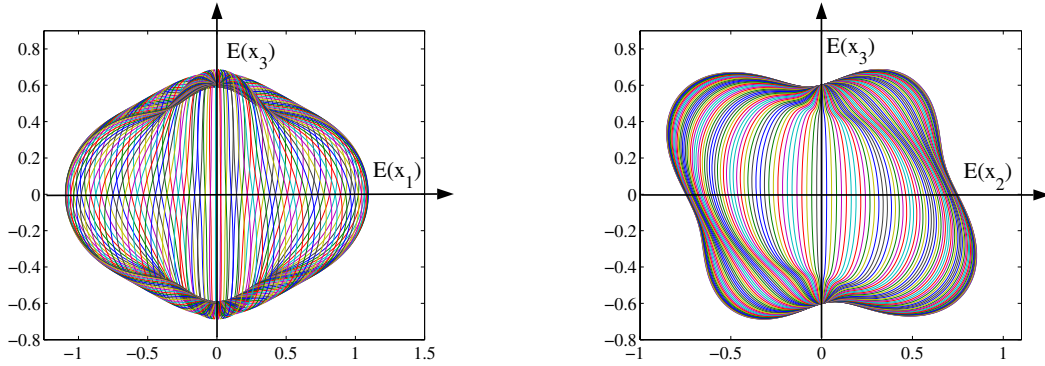
Clearly, we are considering two families of inclusions and a simultaneous approach is not necessary because the inclusions in both subgroups inclusions are identical but differently oriented. Applying the formulae (10-12) for $N = 2$ with tensors $\mathcal{A}_k(z) = \mathbf{R}_k \diamond \mathcal{A}_k(x)$, $k \in \{c1, c2\}$ ³ we obtain results for the stiffness tensor best represented by a monoclinic group. When the axis of reflexive symmetry is $z_1 = x_1$ with invariance under the transformation $x \mapsto x^*$ and $x_1^* = -x_1, x_2^* = x_2, x_3^* = x_3$, the corresponding stiffness tensor (represented by 6×6 symmetric matrix formed by $\{11, 22, 33, 23, 31, 12\} \mapsto \{1, 2, 3, 4, 5, 6\}$) should have the following non-zero terms

$$\mathcal{D}^{app} = \begin{pmatrix} x & x & x & x & 0 & 0 \\ & x & x & x & 0 & 0 \\ & & x & x & 0 & 0 \\ & & & x & 0 & 0 \\ & & & & sym & x \\ & & & & & x \end{pmatrix}.$$

characteristic of a monoclinic group. In order to show the elastic material symmetry we calculated the effective Young modulus as a function of direction by means of $E^{eff}(n) = n \diamond \mathcal{D}^{eff}$. Thus, on figure 5 the ratio of the effective Young modulus and Young modulus of the matrix i.e. $E^{eff}(n)/E_0$ is shown. The figure was obtained calculating correlation tensors $\mathcal{A}_{\Lambda\Pi}$ under the assumption that mutual interactions have the correlation hole shown in figure 4(b) without

³ Here, for brevity of notation $(\mathbf{R} \diamond \mathcal{A})_{\alpha\beta\gamma\delta} \equiv (\mathbf{R})_{\alpha a} (\mathbf{R})_{\beta b} (\mathbf{R})_{\gamma c} (\mathbf{R})_{\delta d} (\mathcal{A})_{abcd}$ is introduced.

overlapping.⁴ The anisotropy factor was estimated to be $\zeta = 0.1669$.



(a) Young modulus for 2-voids with symmetry plane indicated.

(b) Young modulus for 2-voids in symmetry plane view.

Figure 5. Spatial distribution of Young modulus $E^{eff}(n)/E_0$ for originally parallel pores ($c_{c1} = 0.2$ and $c_{c2} = 0.1$) mutually rotated by $\pi/3$.

Example 2.

As another characteristic example, let us again apply the same procedure to an elastomeric matrix composite with short needlelike spheroidal fibres and oblate very thin spheroidal voids modeling cracks. Fibres are characterized by a Young modulus five times larger than the Young modulus of the matrix i.e. $E_f = 5 E_0$ and $c_f = 0.2$ whereas fibres concentration of voids amounts to $c_c = 0.15$. Again the fibres are rotated by some angle θ_1 around axis z_1 whereas the voids are rotated by $\theta_2 = -\theta_1$ around the same axis. The angles $\psi_1 = \psi_2 = 0$ and aspect ratios of both types of inclusions are: $\gamma_c = 1/\gamma_f = a_{c1}/a_{c3} = a_{c2}/a_{c3}$. The composite obtained in such a way again has planar material symmetry along the axis $x_1 = z_1$. Fibres as well as voids in each group are parallel but randomly distributed. By making use of the Boolean random distribution and fibre priority, the application of simultaneous approach (cf. (13-17) in Kanaun-Jeulin approach) leads to explicit values for the effective stiffness tensor. It is informative to graphically represent the effective Young modulus as a function of direction. The ratio $E^{eff}(n)/E_0$ presented in figure 6 and the value $\zeta = 0.1382$ reveals that anisotropy in this case is less pronounced than in the case of two families of oblate voids.

Example 3.

The last case is concerned with reinforcement by means of two families of needlelike fibres with concentrations $c_{f1} = 0.2$ and $c_{f2} = 0.1$ rotated again by $\theta_2 = -\theta_1 = \pi/6$ from their original configuration. Correlations are again calculated by the interaction scheme explained in figure 7. In this case anisotropy is the weakest such that $\zeta = 0.0663$.

Example 4.

It is to be expected that thermal and elastic anisotropy caused by the presence of ellipsoidal inclusions are not the same. To show this we will again calculate the effective thermal expansion tensor for the case explained by the previous example when two families of short fibres are rotated mutually by $\theta_1 = -\theta_2 \in [0, \pi/6]$. For this sake we take that $\alpha_k = \alpha_k \mathbf{1}$, $k \in \{0, f\}$ with values of $\alpha_0 = 5 \times 10^{-6}$ and $\alpha_f = 1 \times 10^{-6}$ for matrix and fibres, respectively.

⁴ Accepted overlapping would correspond to branching and extension of thin voids modeling cracks. This means inelasticity whereas in this paper we are concerned with elasticity only.

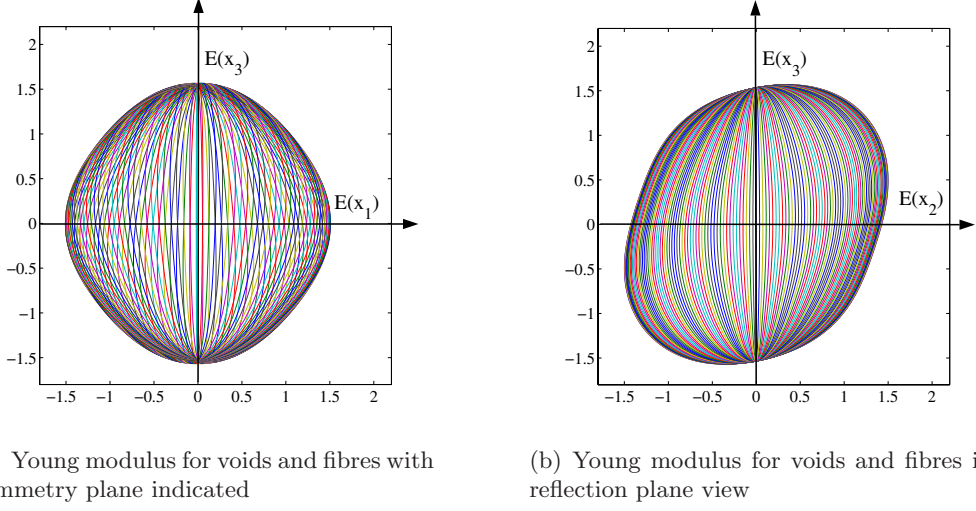


Figure 6. Spatial distribution of Young modulus ($E^{eff}(n)/E_0$) for parallel fibres ($c_f = 0.2$) and pores ($c_c = 0.1$) mutually rotated by $\pi/3$.

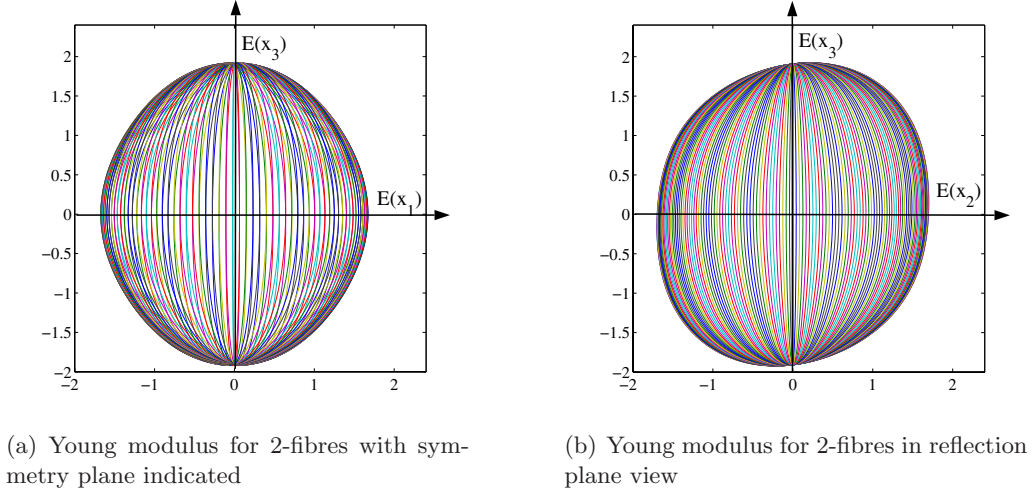


Figure 7. Spatial distribution of Young modulus ($E^{eff}(n)/E_0$) for two families of parallel fibres ($c_{f1} = 0.2$) and ($c_{f2} = 0.1$) mutually rotated by $\pi/3$.

Applying the relationships derived in the subsection 2.2 we found an effective thermal expansion tensor for such a composite. The results of such a calculation are depicted in figure 8(a) by means of the ratio $\alpha_{min}/\alpha_{max}$ of minimal and maximal principal values of the tensor α^{eff} . The continuous line in this figure corresponds to interaction 4-tensors $\mathcal{B}_{\Lambda\Pi}^\Phi$, $(\Lambda, \Pi) \in \{(f, c), (c, f)\}$, calculated by means of (26) and correlation holes with size $\beta := |x|_{max}/|x|_{min} = 1.5$. The same procedure for $\beta = 150$ yields a slightly weaker thermal anisotropy given by the dotted line.

Since the procedure derived in the subsection 2.2 for the effective thermal expansion requires considerable computing time it would be handy to have a shortcut by means of some approximate procedure. Thus, in figure 8(b) the dotted line obtained by means of the approximation $\mathcal{B}_{\Lambda\Pi}^\Phi = 0.001\mathcal{B}_\Lambda$ for $\Lambda = \Pi$ and $\mathcal{B}_{\Lambda\Pi}^\Phi = 0.001 \cos(\theta_1 + \theta_2)\mathcal{B}_\Lambda$ for $\Lambda \neq \Pi$ where $(\Lambda, \Pi) \in \{(f, c), (c, f)\}$ is compared with the continuous line which is the same as continuous line in figure 8(a). Such an approximation is again rather satisfactory. When multiplication is made by factors larger

than 0.001 the deflection is larger. This shows that a self consistent approximation by isolated inclusion might be usable for a composite with two families of short rotated rigid fibres.

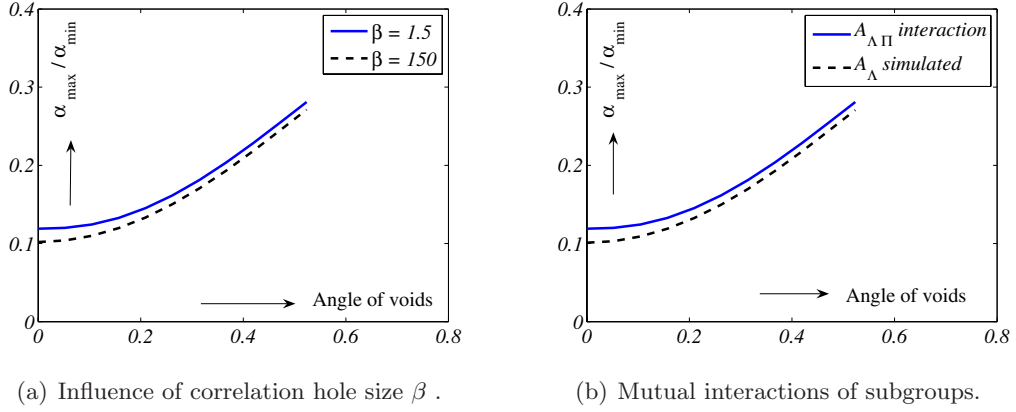


Figure 8. Ratio $\alpha_{min}/\alpha_{max}$ as a measure of thermal anisotropy.

After all these examples let us make a final comment about the effective elastic and thermal symmetry. For the simultaneous embedding of two families of inclusions the effective stiffness is found from the formula (13) in which tensors \mathcal{T}_Λ and \mathfrak{T}_Λ depend on \mathbf{R}_Λ and a_Λ for Λ -inclusions by means of $\mathcal{A}_\Lambda = \mathcal{S}_\Lambda(\mathbf{R}_\Lambda, a_\Lambda)\mathcal{D}_0^{-1}$ (cf. (6)) as well as correlation 4-tensors $\mathcal{A}_{\Lambda\Pi}$ determined either by Kanaun-Jeulin relations (15-17) or by means of the correlation holes presented in figure 4(b). Suppose now that instead of a large disorder angle $\theta_2 = -\theta_1$ a slight disorder of two families of inclusions takes place. Then \mathcal{A}_Λ and $\mathcal{A}_{\Lambda\Pi}$ may be developed into a power series in \mathbf{R}_Λ keeping only linear terms (like in [26] for micromorphic polycrystals). Instead of very low monoclinic symmetry obtained here, such an approach would lead to approximate effective transverse isotropy or some other higher degree of symmetry. A similar comment holds true for the effective thermal symmetry. Such an analysis is planned for a subsequent paper.

Concluding remarks

The results of this paper may be shortly summarized as follows:

- By making use of Kanaun-Jeulin stochastic analysis of the self consistent method (the effective field approach) the effective stiffness 4-tensor as well as the effective thermal expansion 2-tensor are formulated and found numerically. The thermal expansion tensor for two families of ellipsoidal inclusions is derived on the basis of Levin's approach.
- Markov's results for N diverse inclusions with PonteCasteneda-Willis joint correlation tensors are applied with sequential embeddings of inclusions to a composite with two families of voids.
- Dependence of the effective symmetry of the representative volume element on topology and thermoelastic material properties of inclusions is defined and analyzed by means of the effective orientation distribution function. Simultaneous embedding and Kanaun-Jeulin theory are employed with a modification concerning non-random disordered inclusions. The slight disorder case is also discussed.
- Development of damage induces elastic as well as thermal asymmetry and deserves attention when attempting to develop a multiphase self consistent theory.

The main conclusion is that estimation of the effective elastic or thermal symmetry depends on the proposed procedure. For instance an application of the sequential approach with

ordered families of inclusions depends on the chosen order of embedding. This task is easier when concentration of one family is dominant. Such a conclusion calls for an improvement of determination of effective stiffness for composites with more than one class of inclusions as well as a careful extensive additional study of shapes and sizes of correlation holes and corresponding correlation functions.

Acknowledgments

This research has been done within the project MM-144038 financially supported by the Ministry of Science and Technology of Serbia.

References

- [1] Albertini C, Montagnani M and Micunovic M 1989 *Transactions of SMIRT-10* vol L, ed A H Hadjian (Los Angeles: AASMIRT) p 31
- [2] Anthony K-H 1970 *Fundamental Aspects of Dislocation Theory* vol I, ed J A Simmons, R de Wit and R Bullough (Washington D C: National Bureau of Standards Special Publication **317**) p 637
- [3] Bilby E 1960 *Progress in Solid Mechanics* **1** 329
- [4] Boehler J-P 1979 *ZAMM* **59** 157
- [5] Böhlke T and Bertram A 2003 *Comput. Mater. Sci.* **26** 13
- [6] Eshelby J D 1957 *Proc. Roy. Society* **241** 376
- [7] Hill R 1965 *J. Mech. Phys.Solids* **13** 213
- [8] Kachanov M 1980 *J. Engng. Mech. Division* **EM5** 1039
- [9] Kachanov M 1993 *Advances in Applied Mechanics* vol 30, ed J W Hutchinsom and T Wu (New York: Academic) p 259
- [10] Kanaun S K and Kudrjavceva L T 1987 *Izv. ANSSSR Mekhanika Tverdogo Tela* (in Russian) **4** 113
- [11] Kanaun S K and Levin V M 1993 *Effective Field Method in Mechanics of Composites* (in Russian) (Petrozavodsk: Petrozavodsk University Edition)
- [12] Kanaun S K and Jeulin D 2001 *J. Mech. Phys. Solids* **49** 2339
- [13] Kondo K 1958 *RAAG Memoirs* **II(D)** (Tokyo: Gakujutsu)
- [14] Krajcinovic D 1996 *Damage Mechanics* (Amsterdam: Elsevier)
- [15] Kröner E 1960 *Arch. Rational Mech. Anal.*, **4** 273
- [16] Kudrjavceva L, Sumarac D and Micunovic M 2003 *Proc. Yugoslav congress of mechanics* Belgrade
- [17] Kunin I A 1983 *Elastic Media with Microstructure* (Berlin: Springer Series in Solid State Sciences)
- [18] Kunin I A and Sosnina E G 1971 *Doklady Akademii Nauk SSSR* (in Russian) **199/3** 571
- [19] Levin V M 1976 *Izv. ANSSSR Mekhanika Tverdogo Tela (MTT)* (in Russian) **6** 137
- [20] Levin V M 1982 *Appl. Math. Mech. (PMM)* (in Russian) **46/3** 502
- [21] Markov K Z 1995 *Int. J. Engng. Sci.* **33** 139
- [22] Markov K Z 2001 *J. Mech. Phys. Solids* **49** 2621
- [23] Micunovic M 1974 *Bull. Acad. Polon. Sci.,Ser. Sci. Techn.* **22/11** 579
- [24] Micunovic M 1979 *Theoret. Appl. Mech.* **5** 91
- [25] Micunovic M 1992 *Facta Universitatis* **1(2)** 155
- [26] Micunovic M 2002 *Theoret. Appl. Mech.* **28-29** 235
- [27] Micunovic M 2005 *Phil. Magazine* **85 (33-35)** 4031
- [28] Micunovic M 2006 *AMMA* vol III, ed R W Ogden and D Gao (Berlin: Springer) p 187
- [29] Morris P R 2006 *J. Appl. Crystallography* **39/4** 502
- [30] Mura T 1988 *Micromechanics of Defects in Solids* (Dodrecht: Martinus Nijhoff)
- [31] Ponte Castaneda, P. and Willis, J. R., 1995 *J. Mech. Phys. Solids* **43** 1919
- [32] Shermegor T D 1977 *Theory of Elasticity of Micro-inhomogeneous Media* (in Russian) (Moscow: Nauka)
- [33] Sumarac D and Krajcinovic D 1987 *Mech. Materials* **6** 39
- [34] Willis J R 1982 *Mechanics of Solids* ed H G Hopkins and M J Sewell (Oxford: Pergamon) p 653
- [35] Yaguchi M and Busso E P 2005 *Int. J. Solids Structures* **42** 1073